Experimental Astronomy (2023) 55:209–222
https://doi.org/10.1007/s10686-022-09859-4

ORIGINAL ARTICLE

Portraying the missing baryonic mass at the cosmic noon: the contribution of CUBES

Valentina D'Odorico[1,2,3]

Received: 7 October 2021 / Accepted: 6 April 2022 / Published online: 30 April 2022

Abstract

The cosmological and galactic missing baryon problems are briefly reviewed with a particular focus on the contributions to the baryonic census derived from the analysis of quasar absorption spectra. The CUBES spectrograph foreseen for the ESO VLT, with its exceptional efficiency (> 40 %), blue wavelength coverage ($\lambda \simeq 300 - 405$ nm) and intermediate resolution ($R \simeq 24,000$) will allow us to tackle this issue with two approaches: using H I Lyman-α lines at $z \simeq 1.5 - 2.3$, just after the peak of star formation, and using O VI absorbers at $z \simeq 1.9 - 2.9$, at the cosmic noon. In both cases, in order to derive the baryonic masses it will be necessary to acquire also higher-resolution spectra of the same target quasars to cover the region at longer wavelengths. We simulate the observations with the CUBES E2E simulator considering a sample of 40 bright quasars at redshifts $z_{\rm em} \sim 2 - 3$ observed for a total time of ~ 13 h to reach a signal-to-noise ratio of ~ 15 in the H I Lyman-α, O VI forests.

Keywords Intergalactic medium · Circumgalactic medium · Quasars: absorption lines · cosmology: observations

1 Introduction

The early universe was a highly uniform and homogeneous mix of dark and baryonic matter. The ratio between these two components as predicted by Big Bang Nucleosynthesis [10] and inferred from density fluctuations of the cosmic microwave background [19, 41] is $f_b = \Omega_b/\Omega_m \simeq 0.16$. This primordial mix is expected to persist as large scale structure evolves and individual gravitationally bound objects emerge

✉ Valentina D'Odorico
valentina.dodorico@inaf.it

[1] INAF - Osservatorio Astronomico di Trieste, Via Tiepolo 11, I-34143 Trieste, Italy

[2] Scuola Normale Superiore, Piazza dei Cavalieri 7, I-56126 Pisa, Italy

[3] IFPU - Institute for Fundamental Physics of the Universe, Via Beirut 2, 34014 Trieste, Italy

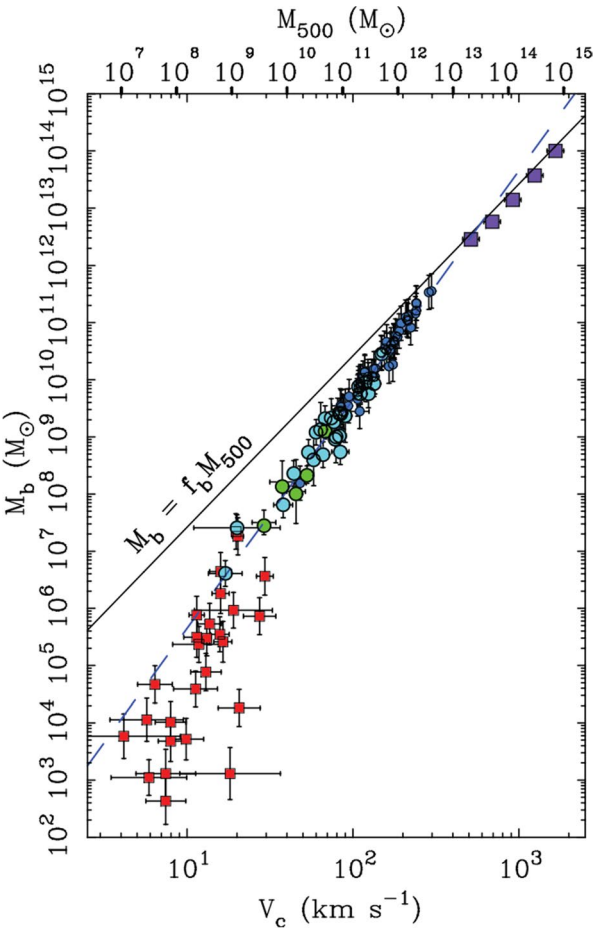

Fig. 1 Relation between baryonic mass and rotation velocity for galaxies. Red squares represent Local Group dwarf satellites. Round symbols represent rotationally supported disks. Purple squares represent the mean of many galaxy clusters. If structures possessed baryons in the cosmic fraction, they would fall on the solid line. The dashed line represents the Baryonic Tully–Fisher relation defined by the disks. Reproduced from [28] by permission of the AAS

during the course of cosmic time. In this hypothesis, the baryonic mass of any given cosmological structure would be $M_b = f_b M_{\rm tot}$.

On the other hand, direct measurements reveal that at $z \sim 0$ a baryonic fraction of $\sim 30 - 40$ % is missing on cosmological scales (e.g. [11, 50]) and also galaxies are baryon deficient. The amount of missing baryons in galaxies depends on the mass/scale of the system: while clusters are in agreement with the primordial fraction, in galaxies outside of clusters we are missing more than 60% of the baryons, rising to ≥ 90 % for gas-dominated galaxies and dwarfs[1] (e.g. [28], see Fig. 1).

Where are the missing baryons? Cosmological, hydrodynamical simulations (e.g. [7, 8, 14, 27, 53, 57]) predict that, at $z \sim 0$, most of the baryons are in the form of unvirialized, diffuse gas: $40 - 50$% have been shock heated by the processes of structure formation and resides in the warm-hot intergalactic medium (WHIM)

[1] The baryonic mass in galaxies is defined as the sum of the stellar plus the cold gas components, $M_b = M_* + M_g$.

characterized by temperatures of 10^5 K $< T < 10^7$ K. Another $30-40$ % is in the diffuse warm medium at $T < 10^5$ K. The cold gas and stars in galaxies contribute less than ~ 20 % and the very hot gas with $T > 10^7$ K (the normal X-ray emitting gas, predominantly in collapsed and virialized clusters of galaxies) gives a negligible contribution. As we move back in time, the warm diffuse component becomes increasingly important and, at $z \gtrsim 2$, it is expected to be the dominant reservoir of baryons for galaxy formation: the intergalactic medium (IGM). The WHIM is predicted to reside mainly in the filaments of the cosmic web where also galaxies lie, connecting the two scales of the missing baryon problem (Fig. 2).

The aim of this paper is: to report on the state-of-the-art of the observations that at $z < 1$ have investigated the contribution to the baryon fraction of the different gaseous components (Sect. 2) and, to describe what is known and what is foreseen for the future on the quest for baryons at higher redshift (Sect. 3), with a particular focus on the measurements that will be enabled by the CUBES spectrograph (Sect. 3.2).

2 A census of baryons at low redshift

2.1 Measurements in the FUV

In order to estimate the contribution to the local baryon budget of the gas outside galaxies, the main observational technique has been far ultra-violet (FUV) spectroscopy of bright background sources.

The H I Lyman-α absorption lines, forming the so called Lyman-α *forest* observed in quasar spectra, are known to probe the neutral component of the diffuse, ionized IGM at temperature $T \sim 10^{3.5} - 10^{4.5}$ K [29]. [50] carry out a detailed study of a sample of 746 H I absorbers observed with STIS/HST from the catalogue compiled by [54]; they apply ionization corrections determined both analytically and from numerical simulations and derive a contribution to the baryon budget $\Omega_b^{(HI)} = 28\% \pm 11\%$[2] in agreement with simulation predictions and previous measurements (e.g. [23]).

The FUV lines due to the O VI doublet ($\lambda\lambda$ 1031.9, 1037.6 Å) are currently the best available tracers of the ''cooler'' portion of the shock-heated gas forming the WHIM, reaching a peak ionization fraction, $f_{\rm OVI} \approx 0.22$, at temperature $T_{\rm max} = 10^{5.45}$ K in collisional ionization equilibrium [52] and similar values in non-equilibrium cooling [18]. Surveys based on FUSE, STIS/HST and COS/HST data assuming fixed metallicity, $Z/Z_\odot = 0.1$, and ionization correction $f_{\rm OVI} = 0.2$, obtained a contribution to the baryon fraction of $\sim 8-9$ % (e.g. [13, 54, 55]). Using simulations to determine a more reliable value of the product of metallicity and ionization fraction, [50] derive a column-density-weighted mean of $f_{\rm OVI}(Z/Z_\odot) = 0.01$, a factor of two smaller than previously assumed. This implies, $\Omega_b^{(OVI)} \simeq 17 \pm 4$ % summing up to the WHIM census in the temperature range $T \sim 10^{5.3} - 10^{5.7}$ K.

[2] The closure parameter at $z = 0$ is defined as $\Omega_b = \rho_b(0)/\rho_{cr}(0)$ and $\rho_b(z) = \rho(0)\,(1+z)^3$.

There are however two main uncertainties affecting this measurement: the value of the gas metallicity that could be larger (e.g. [24, 55]), implying a lower baryon content and, in particular, the fact that O VI absorbers are subject to different physical conditions tracing both collisionally and photo-ionized gas [55]. Since the latter is also traced by the Lyman-α forest, considering all O VI absorbers could amount to a certain degree of double counting.

Unfortunately, a precise determination of the metallicity of O VI absorbers is generally hampered by the scarcity of other associated metal lines. Furthermore, if the missing baryons are predominantly located in gas that is shock heated when it first accreted into galaxy potential wells, then the WHIM plasma could have a relatively low metallicity, and O VI could be difficult to detect in currently available data. An alternative route to detecting WHIM absorbers, and one that does not rely upon metal enrichment, is to detect and measure broad Lyman-α absorbers (BLAs) in high-signal-to-noise ratio spectra. Absorption line width is usually denoted in terms of the corresponding Doppler parameter $b \equiv FWHM/2\sqrt{ln2} \equiv \sqrt{2}\sigma$ where σ is the Gaussian width. The thermal width, which contributes to the total line width, is simply a function of gas temperature T and atomic mass A:

$$\begin{aligned} b_{\rm th}(T) &= \sqrt{2kT/m} = \sqrt{T/60A}\ {\rm km\ s^{-1}} \\ &= (40.6\ {\rm km\ s^{-1}})\, T_5^{1/2} A^{-1/2}, \end{aligned} \tag{1}$$

where T_5 is temperature in units of 10^5 K. BLAs are defined as Lyman-α absorption lines with $b \geq 40$ km s^{-1} and depending on the total gas column density of the WHIM absorber and its temperature, they could have column densities $12.5 \leq \log N$ (H I) ≤ 14. The quantitative estimate of the baryon content of the BLAs is complicated by the effect of non-thermal line broadening processes, line blends, and noise features that can mimic broad spectral troughs. Observational studies report relatively reliable lower limits of $6-10$ % increasing to $\approx 14-20$ % when corrected with simulations [12, 23, 46, 47].

2.2 Measurements in the soft X-rays

Observations in the FUV probe WHIM temperatures up to maximum $T \sim 10^{5.7}$ K. The hot phase of the WHIM can be investigated through absorptions of ionized metals in the soft X-rays [3]. In this energetic regime the most promising ionic transitions are O VII (21.60 Å) and O VIII (18.97 Å) since they are strong transitions of an abundant element with peak collisional ionization equilibrium (CIE) abundances at temperatures of $(12) \times 10^6$ K. Other metal transitions that could be detected in absorption in the X-rays (note that this list is by no means complete) are N VII λ 24.78 Å, Ne IX λ 13.45 Å, and the Lyman-β line of O VII at 18.63 Å.

The mostly used tracers of this WHIM phase are the O VII Heα absorption lines; these are predicted to be relatively narrow (with a Doppler parameter thermal component $b_{\rm th} \approx 20-46$ km s^{-1}), extremely shallow (rest-frame equivalent widths, EW ≤ 10 mÅ) and rare [8, 14]. Current X-ray spectrometers, XMM-Newton and Chandra, do not resolve such lines and thus need a signal-to-noise ratio per resolution element greater than or equal to ~ 20 in the continuum to detect them at a

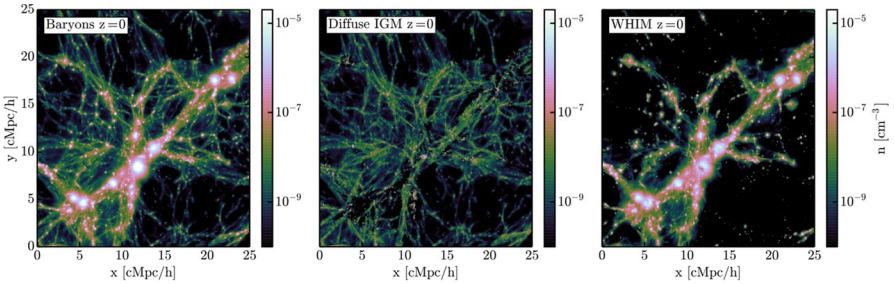

Fig. 2 Projected number density of a filament in a slice of dimensions $25 \times 25 \times 8$ cMpc^3 h^{-3} at redshift $z = 0$. Left-hand panel: all baryons. Centre: diffuse IGM. Right: WHIM. By visual inspection, we see that the diffuse IGM is ubiquitous, whereas the WHIM is concentrated near knots and filaments. Adapted from [27]

significance level exceeding $\sim 3\sigma$. Although substantial observational efforts have been carried out in the last 10 years to target the rare brightest sources at $z \geq 0.3$, no firm, high-significance detections have been reported up to now (see [36] for a recent review). Even the most recent claim of a double detection of O VII at $z = 0.3551$ and $z = 0.4339$ [35] has been subject to revisions that decreased its reliability [21, 34].

The full exploitation of the soft X-ray metal absorption lines to investigate the nature of the WHIM will have to wait for the next generation of instruments, in particular the X-ray integral field unit spectrometer (XIFU: [1]) on board the Athena observatory[3], which is due for launch in the early 2030s.

2.3 Accounting for baryons in galaxy halos

The baryon mass estimates described in the previous sections are based on surveys of absorption lines tracing different environments: from the diffuse IGM, to filaments in the cosmic web and the outskirts of galaxies.

Combining absorption line studies with the identification of galaxies in the field of the background source allows us to investigate the galactic halo properties. The gaseous halo extending out to the virial radius and beyond – dubbed circumgalactic medium (CGM) – is where a large fraction of the baryons missing from galaxies is expected to reside (e.g. [7]). (Fig. 2).

Several studies have shown that the CGM is a major reservoir of heavy elements with a mass rivaling and possibly exceeding that within galaxies [39, 56, 59]. Metals have to be transported from the ISM to ~ 100 kpc distances in the CGM and to attain this goal several mechanisms have been proposed including galactic winds, active galactic nucleus (AGN) feedback, accretion, tidal stripping, and ram pressure. The detailed study of the metallicity and ionization state of the CGM is of great importance to establish which one of those mechanisms was more relevant for the enrichment. Furthermore, heavy element ions are critical to

[3] https://www.the-athena-x-ray-observatory.eu/

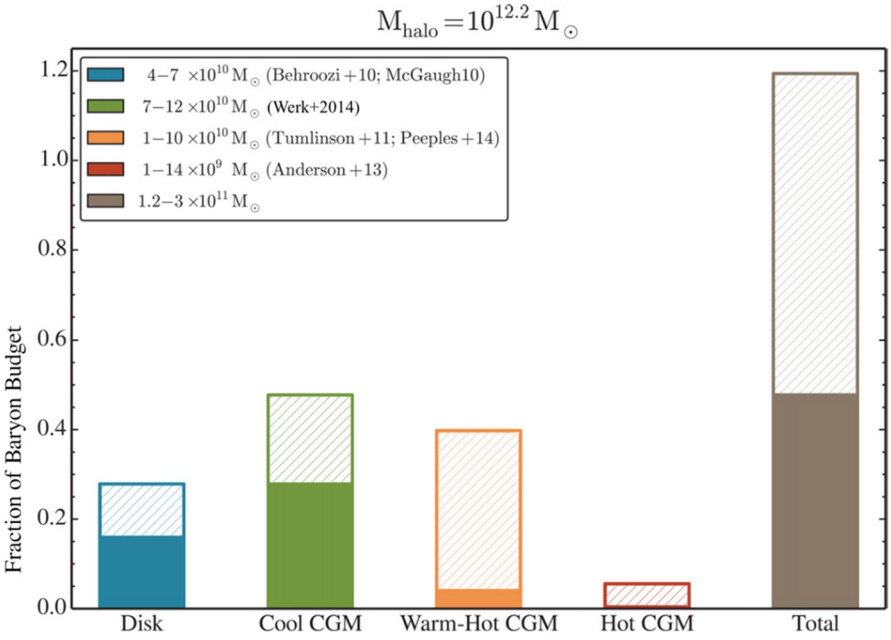

Fig. 3 Baryonic budget of the fiducial COS-Halos galaxy, at $L \approx L_*$, represented as a bar chart showing the most massive baryonic components of the galaxy. The solid filled bars are lower limits to the fraction each component will contribute, while the hatched area above the solid bars shows potential additional contributions allowed by the data. The sum of these components is given by the brown bar, illustrating that galaxies have anywhere between 45% and 100% of their baryons relative to the cosmological fraction. Adapted from [59] and reproduced by permission of the AAS

establish which ionization corrections have to be applied to the measured neutral hydrogen column density (N(H I)) to infer the total gaseous halo mass.

An estimate of the baryon content of the CGM at $z \sim 0$ has been carried out in particular in the context of the COS-Halos survey [60], which investigated the halo properties of a sample of $L \approx L_*$ galaxies whose angular offsets from quasar sightlines and photometric redshifts implied impact parameters ($R < 160$ kpc) well inside their virial radii.

Thanks to the detection in COS spectra of low and intermediate-ionization absorption lines of heavy elements, together with the corresponding H Iabsorption lines, it was possible to assess the physical conditions and mass of highly ionized, cool ($T \approx 10^4$ K) CGM gas observed within 160 kpc of 33 low-redshift, $L \approx L_*$ galaxies [59]. The derived contribution of the cool CGM to the baryonic budget ($0.16\,M_{\rm halo}$) ranges between 25% and 45% (see Fig. 3). Note that this determination is subject to significant uncertainties [44]. On the one hand, several systems had an uncertain determination of the H Icolumn density due to the lack of spectral coverage of the whole Lyman series: the precise measurement of N(H I) is critical for the determination of the halo mass. On the other hand, the very simplified standard photoionization models applied to determine the ionization

correction are known to fail when a wider set of metal ions is considered, suggesting a complex density structure and/or additional ionization mechanisms. More sophisticated models should be developed to reproduce the ionization structure observed in the CGM.

As described in Sect. 2.1, the O VI absorption doublet is the most commonly used tracer of the WHIM gas, being one of the few ions easily observed at rest wavelength $\lambda_r > 912$ Å with ionization potential (IP) $\gtrsim$100 eV. However, discriminating between photoionized and collisionally ionized O VI has proved to be difficult (e.g. [58]). The COS Absorption Survey of Baryon Harbors (CASBaH) obtained high spectral resolution COS/HST and STIS/HST spectra of nine FUV-bright quasars at $0.92 < z_{em} < 1.48$ without known Lyman Limit systems, in order to access transitions at $\lambda_r < 912$ Å. The quasar spectra are complemented by a survey for galaxies in the fields surrounding the nine sightlines, for a total of ~ 5900 galaxies whithin ≈ 10 comoving Mpc [42]. A goal of the CASBaH survey was to investigate the presence of the Ne VIII $\lambda\lambda$ 770.41, 780.32 Å doublet in the CGM of galaxies close to the line of sight. With IP = 207 eV, Ne VIII can persist in gas with $10^5 < T < 10^6$ K, and thereby complements O VI with the potential to break degeneracies in ionization models. [4] detected Ne VIII associated with 9 galaxies of the 29 that they could consider for their experiment. They estimated the mass in Ne VIII-traced gas to be $M_{gas}(\text{Ne VIII}) \geq 10^{9.5} M_{\odot} (Z/Z_{\odot})^{-1}$, or 6%–20% of the expected baryonic mass depending on the Ne VIII absorbers' metallicity. This estimate assumes the peak of the ionization fraction, Ne VIII/Ne, under collisional ionization, or $T \sim 10^{5.8}$ K. Interestingly, this is similar to the virial temperature for the median halo mass and redshift ($\langle z \rangle = 0.68$) of their sample, implying that the Ne VIII-bearing gas is plausibly collisionally ionized near this temperature.

2.4 Is the missing baryon problem solved?

Recently, a new astronomical phenomenon has been discovered: the fast radio bursts (FRB), radio flashes of unknown physical nature with duration of milliseconds. The dispersion measure (DM) of a short and coherent burst of radiation from a distant source offers an integral constraint on the electron distribution along the path between the source and the Earth. This includes the IGM, our Galaxy, our Local Group, the galaxy hosting the FRB, and the baryons residing in other galactic haloes near the sightline (e.g. [30, 43, 49]).

Thanks to the repeatability of some of these FRB it has been possible to localize them and associate them with galactic counterparts (e.g. [9]).

[25] have recently exploited the dispersion observed in a sample of localized FRB at $z \sim 0.1 - 0.5$ to measure the electron column density and account for every ionised baryon along the line of sight. This independent measurement of the baryon content of the Universe with a golden sample of five FRBs is consistent with the CMB and Big Bang Nucleosynthesis values, substantially solving the missing baryon problem at low redshift.

This result has established the total amount of baryons, confirming that they are distributed in several environments. However, with the present sample of localized

FRB it is not possible to distinguish the share of the different gaseous components. In this respect, quasar absorption lines studies will continue to play a key role, in particular, they could help understand whether a substantial fraction of the mass at high redshift is also contained in diffuse halo components.

3 Baryons in the high redshift IGM/CGM

At $z \sim 3$ most of the baryons (~ 90 %) are in the diffuse IGM which is traced by the Lyman-α forest [16, 45]. Also the diffuse gas in the halo of galaxies is expected to contribute significantly to the total budget, hosting the (metal enriched) gas expelled from galaxies by stellar and AGN feedback processes and also the gas accreting from the IGM to fuel the star formation (e.g. [38]). The contribution of the warm-hot gas to the baryon census at $z \sim 2.5$ was determined in [51] by studying the O VI absorbers along 5 lines of sight observed with HIRES at Keck. They found that these systems arise at the interface between the IGM and galaxies, in the CGM, and that they contribute ≥ 5 % to Ω_b. A very similar experiment was carried out by [6] with 2 lines of sight observed with UVES/VLT, probing O VI absorbers at $z \sim 2$. These authors found that gas traced by O VI represent ~ 20 % of Ω_b, implying a large uncertainty in this determination. [22] investigated the baryonic content of the CGM as traced by absorbers optically thick at the Lyman limit (characterized by column densities $N(\mathrm{H\,I}) \geq 10^{17}$ cm^{-2}) at $z \sim 2-3$. They determined the metallicity of the absorbers, which is critical to estimate the ionized fraction of the gas (since the ionized gas is only observed via the metal lines) and obtained that highly ionized gas in the $\tau_{\mathrm{LL}} > 1$ absorbers is very likely the second largest contributor after the Lyman-α forest to the baryon budget at $z \sim 2-3$ and also a substantial contributor to the metal budget. This work was based on 22 quasar spectra obtained with the HIRES/Keck spectrograph and selected from the 1st data release of the KODIAQ survey [37]. The considered spectra are characterized by slightly different resolutions and signal-to-noise ratios in the O VI forest varying from 6 to 54. To our knowledge there are no other recent studies that dealt with the determination of the baryonic content of the $z \gtrsim 2$ CGM and we think that further investigations are needed based on homogeneous and unbiased samples of quasar spectra. We note that a good coverage and, in particular, a large efficiency in the UV region of the spectrum is essential to cover more transitions in the Lyman series and determine with greater accuracy the H Icolumn density, from which the halo mass is derived.

3.1 Future measurements

Several current and future instruments are being designed with the study of the high-redshift ($z \gtrsim 2$) CGM in mind. One of the cases developed for the ELT-MOSAIC instrument ([48], see Fig. 4 and note that the goal is to extend the visible coverage of MOSAIC down to 390 nm) is to use high-redshift Lyman-break galaxies as background sources to reconstruct the 3D density field of the IGM and probe the CGM of galaxies at $z \sim 3$ [20]. The Keck Cosmic Web Imager (KCWI) instrument [32], commissioned in 2018, has partly been designed to address this topic and will certainly

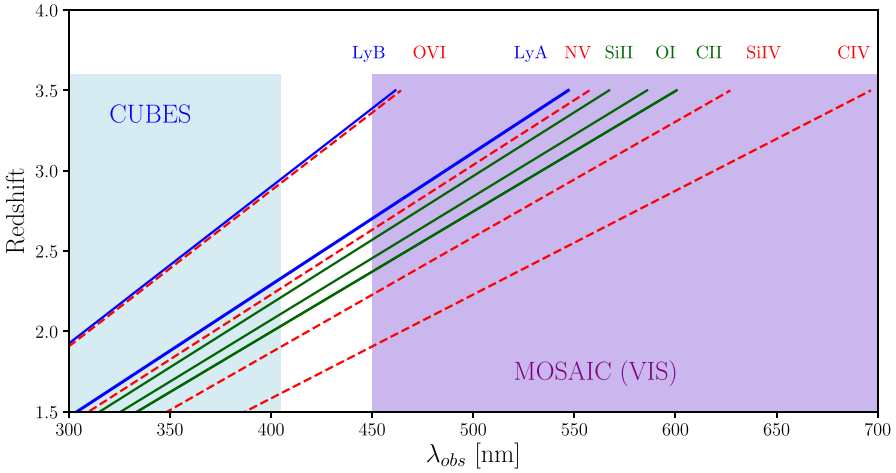

Fig. 4 Lines available in the ground-UV for studies of the CGM of galaxies at $1.5 < z < 2.3$ (or $1.9 < z < 2.9$ for O VI absorbers). They span a range of ionisation states (green = low, red = high) to study the relative fractions of cold vs. warm vs. hot gas, at redshifts where the contamination of key ions such as O VI by the Lyman-α forest is less severe. CUBES observations will neatly complement future observations in the blue-visible with ELT-MOSAIC, which is targeting the CGM in galaxy halos at $z \sim 3$

make significant contributions, but its blueward coverage stops at 350 nm. Observations in the ground-UV can play an exciting role in this field, considering also the fact that, with the present design, the ELT will be almost blind at $\lambda \lesssim 400$ nm.

The CUBES spectrograph, foreseen for the ESO VLT, has been designed to be extremely efficient (> 40 %) in the wavelength range $\lambda \sim 300 - 405$ nm with a resolving power $R \simeq 24,000$ [61] and with the possibility to have a fiberlink connection with the UVES/VLT spectrograph to cover simultaneously the region at $\lambda > 420$ nm. These characteristics, makes CUBES an ideal instrument to carry out further investigations of the cosmological baryonic mass content and of the contribution to the baryonic budget of the CGM in redshift regimes not particularly explored before, as we describe in the next section.

3.2 The CUBES baryon experiment

The spectral properties of CUBES allow us to foresee two experiments for the measure of the baryonic mass with quasar absorption lines. In the first one, the baryons in the diffuse IGM will be chased through the detection and analysis of H I Lyman-α absorption lines at $z \simeq 1.5$ to 2.3 (see Fig. 4). This redshift range, immediately after the era of peak star-formation in the Universe (e.g. [26]), is poorly investigated due to observational difficulties (namely the low efficiency of ground-based spectrographs in the UV) but critical to connect the low and high redshift results. The relatively low number density of lines in the Lyman-α forest at these redshifts implies that, even with observations at $R \sim 24,000$, the impact of blending with metal lines in the Lyman-α forest can be minimised (which is not the case at larger redshifts). To complement the information on the neutral IGM component derived from the

Lyman-α forest, we will need to check also the associated metal absorption lines (in particular due to C IV and Si IV) and derive the contribution of the ionised gas. To this purpose, UVES/VLT (or ESPRESSO/VLT) spectra of the same targets will have to be obtained (or retrieved from the ESO archive) to cover the wavelength range at $\lambda > 405$ nm at higher resolution.

In the second experiment, we will use the important O VI absorption line at $1.9 < z < 2.9$ to trace the warm-hot gas at $T > 10^5$ K, associated with the IGM (e.g. [11]) or with the CGM, using the approach described in [22]. Also in this case, CUBES observations will need complementary UVES (or ESPRESSO) spectra to complete the coverage of the associated H I and metal transitions.

Based on previous works, we estimated the time necessary to carry out the CUBES baryon experiments with a sample of ~ 40 bright quasars at redshifts $z_{\rm em} \sim 2-3$.

For our purpose, we want to be sensitive at $3\,\sigma$ to H I Lyman-α lines with column density N(H I) $\gtrsim 10^{12.5}$ cm^{-2} and to O VI 1031 Å absorption lines with N(O VI) $\gtrsim 10^{13}$ cm^{-2}, these thresholds correspond[4] to a signal-to-noise ratio $SNR \sim 15$ per pixel of 0.006 nm at 313 nm (increasing to $SNR \sim 22$ if aiming at the detection of BLA with $b = 40$ km s^{-1}).

We used the CUBES E2E simulator [17] with the custom composite quasar spectrum *QSO_composite_absorbed.dat* with a superposed Lyman-α forest, and simulated observations carried out three days from new moon (Fig. 5). Considering an ideal sample formed by 10 targets at $z_{\rm em} = 2$, 20 at $z_{\rm em} = 2.5$ and 10 at $z_{\rm em} = 3$, all with a conservative magnitude u(AB) = 18, we derived that observing times of 900s ×2, 600s ×2 and 300s ×3 are necessary at the three considered redshifts to reach the desired signal-to-noise ratio in the Lyman-α and O VI forests, summing up to a total exposure time of ~ 13 hours.

We note that in the SQUAD sample [33], compiled from UVES archival quasar spectra, there are ~ 40 targets with $2 \leq z_{\rm em} \leq 3$ and signal-to-noise ratio $SNR \geq 20$ at 350nm (13 with $SNR \geq 40$), covering the wavelength range 305-400nm, although not always completely. We plan to use these spectra (and others with similar wavelength coverage and SNR from KODIAQ, if available) for a preparatory work that will allow us to determine the optimal number and redshift distribution of targets for the CUBES experiments.

The ongoing QUBRICS survey [2, 5] which identifies quasars in the southern hemisphere with i(AB) < 18 mag, will provide the bright targets needed for this case.

4 Conclusions

It is almost thirty years that scientists look for a definitive answer to the question "Where are the baryons?" (e.g. [16, 40]). Today, we can probably state that all the baryons predicted by the CMB and Big-Bang nucleosynthesis measurements have

[4] We used equations 2 and 3 in [15] assuming a Doppler parameter $b = 15$ (10) km s^{-1} for H I(O VI) lines.

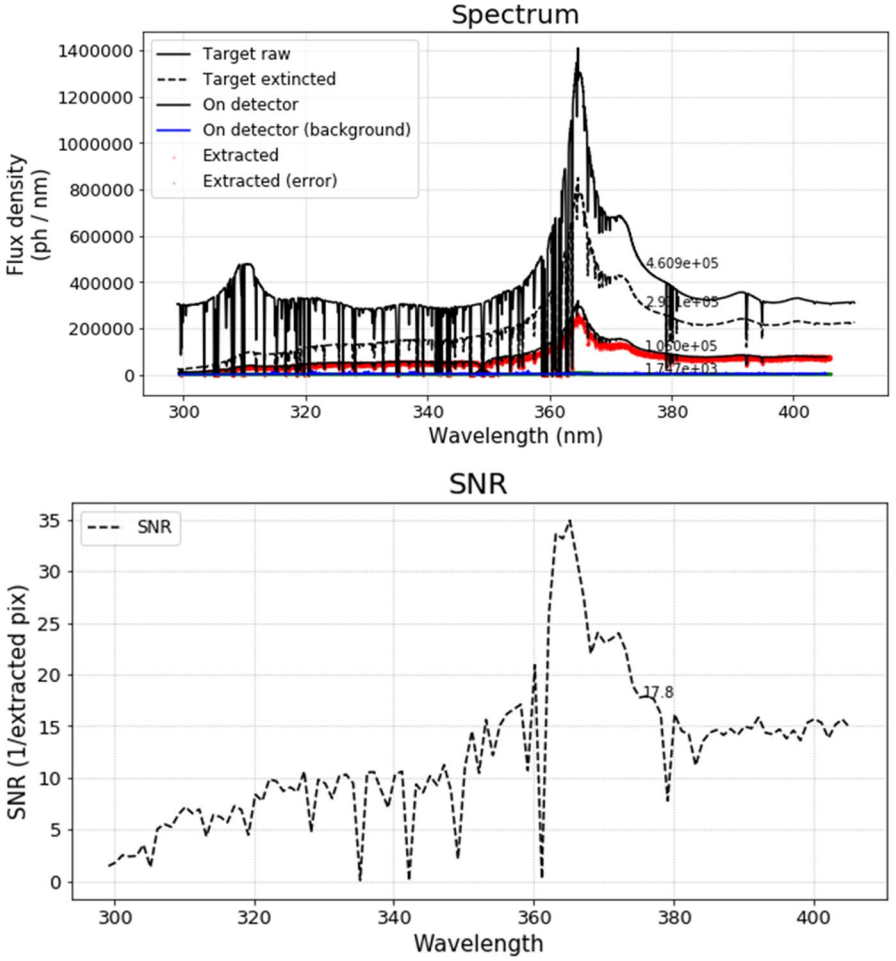

Fig. 5 Output of the E2E simulator for the case of a quasar at $z_{em} = 2.5$ with magnitude $u(\mathrm{AB}) = 18$ observed for 600s. The *upper panel* shows the input spectrum (solid black line, *target raw*), the input spectrum with atmospheric extinction (dashed black line, *target extincted*), the spectrum that is seen by the detector, i.e. scaled by telescope and instrument efficiency (solid black line, *on detector*), the background seen on the detector (solid blue line, *on detector background*), the spectrum recovered by simple (non-optimal) extraction (red dots, *extracted*), the error on the extracted spectrum (green dots, *extracted error*). In the *lower panel* the signal-to-noise ratio per pixel is reported

been detected: at low redshifts thanks to the dispersion measure in FRBs [25], at $z \gtrsim 2$ based on the Lyman-α forest observations and simulations (e.g. [31]). This settled, the next step is to investigate in details how baryonic matter is distributed among the different gaseous components with the aim of understanding and constraining the mechanisms that determined the observed distribution (stellar and AGN feedback, accretion, etc.).

The CUBES spectrograph, with its exceptional efficiency in the UV and relatively high resolution, will play a critical role on these issues, in particular it will allow us

to dig into the complex nature of the inter and circum-galactic gas at $z \sim 1.5 - 3$. For reference, we determined that an exposure time of $\sim$ 13 hours would be needed with CUBES to observe a sample of $\sim$ 40 bright background quasars at $z_{\rm em} \sim 2 - 3$, reaching the necessary signal-to-noise ratio for the proposed science case. Its improved performances with respect to UVES/VLT will open up background sources 1-2 magnitudes fainter than the quasars used at present, significantly increasing the number (and the space density) of available targets and/or the possibility to obtain very high signal-to-noise ratio spectra to detect the faint lines (e.g. [15]).

Acknowledgements VD thanks Stefano Cristiani for useful discussions and a careful reading of the draft, and Guido Cupani for the support in the use of the E2E simulator.

Funding Open access funding provided by Istituto Nazionale di Astrofisica within the CRUI-CARE Agreement.

Data Availability All data mentioned in the paper (e.g. the SQUAD and KODIAQ databases) are publicly available.

Declarations

Conflict of interest The author declare that she has no conflict of interest.

References

1. Barret, D., Lam Trong, T., den Herder, J.-W., et al.: The Athena X-ray Integral Field Unit (X-IFU). SPIE **9905**, 99052F (2016)
2. Boutsia, K., Grazian, A., Fontanot, F., et al.: The Luminosity Function of Bright QSOs at z ∼ 4 and Implications for the Cosmic Ionizing Background. ApJ **912**, 111 (2021)
3. Bregman, J.N.: The Search for the Missing Baryons at Low Redshift. ARA&A **45**, 221–259 (2007)
4. Burchett, J.N., Tripp, T.M., Prochaska, J.X., et al.: The COS Absorption Survey of Baryon Harbors (CASBaH): Warm-Hot Circumgalactic Gas Reservoirs Traced by Ne VIII Absorption. ApJL **877**, L20 (2019)
5. Calderone, G., Boutsia, K., Cristiani, S., et al.: Finding the Brightest Cosmic Beacons in the Southern Hemisphere. ApJ **887**, 268 (2019)
6. Carswell, B., Schaye, J., Kim, T.-S.: The Enrichment History of the Intergalactic Medium: O VI in Lyα Forest Systems at Redshift z∼2. ApJ **578**, 43–59 (2002)
7. Cen, R., Ostriker, J.P.: Where Are the Baryons? II. Feedback Effects, ApJ **650**, 560–572 (2006)
8. Cen, R., Ostriker, J.P.: Where Are the Baryons? ApJ **514**, 1–6 (1999)
9. Chatterjee, S., Law, C.J., Wharton, R.S., et al.: A direct localization of a fast radio burst and its host. Natur **541**, 58–61 (2017)
10. Cooke, R.J., Pettini, M., Steidel, C.C.: One Percent Determination of the Primordial Deuterium Abundance. ApJ **855**, 102 (2018)

11. Danforth, C. W., Keeney, B. A., Tilton, E. M., et al., An HST/COS Survey of the Low-redshift Intergalactic Medium. I. Survey, Methodology, and Overall Results, ApJ, 817, 111 (2016)
12. Danforth, C.W., Stocke, J.T., Shull, J.M.: Broad H I Absorbers as Metallicity-independent Tracers of the Warm-Hot Intergalactic Medium. ApJ **710**, 613–633 (2010)
13. Danforth, C. W., & Shull, J. M., The Low-z Intergalactic Medium. III. H I and Metal Absorbers at z < 0.4, ApJ, 679, 194-219 (2008)
14. Davé, R., Cen, R., Ostriker, J.P., et al.: Baryons in the Warm-Hot Intergalactic Medium. ApJ **552**, 473–483 (2001)
15. D'Odorico, V., Cristiani, S., Pomante, E., et al.: Metals in the z ∼ 3 intergalactic medium: results from an ultra-high signal-to-noise ratio UVES quasar spectrum. MNRAS **463**, 2690–2707 (2016)
16. Fukugita, M., Hogan, C.J., Peebles, P.J.E.: The Cosmic Baryon Budget. ApJ **503**, 518–530 (1998)
17. Genoni, M., Landoni, M., Cupani, G. et al., The CUBES Instrument model and simulation tools, ExA, in press as part of the CUBES Special Issue
18. Gnat, O., Sternberg, A.: Time-dependent Ionization in Radiatively Cooling Gas. ApJS **168**, 213–230 (2007)
19. Hinshaw, G., Larson, D., Komatsu, E., et al.: Nine-year Wilkinson Microwave Anisotropy Probe (WMAP) Observations: Cosmological Parameter Results. ApJS **208**, 19 (2013)
20. Japelj, J., Laigle, C., Puech, M., et al.: Simulating MOS science on the ELT: Lyα forest tomography. A&A **632**, A94 (2019)
21. Johnson, S.D., Mulchaey, J.S., Chen, H.-W., et al.: The Physical Origins of the Identified and Still Missing Components of the Warm-Hot Intergalactic Medium: Insights from Deep Surveys in the Field of Blazar 1ES1553+113. ApJL **884**, L31 (2019)
22. Lehner, N., O'Meara, J. M., Fox, A. J., et al., Galactic and Circumgalactic O VI and its Impact on the Cosmological Metal and Baryon Budgets at $2 < z \lesssim 3.5$, ApJ, 788, 119 (2014)
23. Lehner, N., Savage, B. D., Richter, P., et al., Physical Properties, Baryon Content, and Evolution of the Lyα Forest: New Insights from High-Resolution Observations at $z \lesssim 0.4$, ApJ, 658, 680-709 (2007)
24. Lehner, N., Savage, B.D., Wakker, B.P., Sembach, K.R., Tripp, T.M.: Low-Redshift Intergalactic Absorption Lines in the Spectrum of HE 0226–4110. ApJS **164**, 1–37 (2006)
25. Macquart, J.-P., Prochaska, J.X., McQuinn, M., et al.: A census of baryons in the Universe from localized fast radio bursts. Natur **581**, 391–395 (2020)
26. Madau, P., Dickinson, M.: Cosmic Star-Formation History. ARA&A **52**, 415–486 (2014)
27. Martizzi, D., Vogelsberger, M., Artale, M.C., et al.: Baryons in the Cosmic Web of IllustrisTNG - I: gas in knots, filaments, sheets, and voids. MNRAS **486**, 3766–3787 (2019)
28. McGaugh, S.S., Schombert, J.M., de Blok, W.J.G., Zagursky, M.J.: The Baryon Content of Cosmic Structures. ApJL **708**, L14–L17 (2010)
29. McQuinn, M.: The Evolution of the Intergalactic Medium. ARA&A **54**, 313–362 (2016)
30. McQuinn, M.: Locating the "Missing'' Baryons with Extragalactic Dispersion Measure Estimates. ApJL **780**, L33 (2014)
31. Miralda-Escudé, J., Cen, R., Ostriker, J.P., Rauch, M.: The Ly alpha Forest from Gravitational Collapse in the Cold Dark Matter + Lambda Model. ApJ **471**, 582 (1996)
32. Morrissey, P., Matuszewski, M., Martin, C., et al., The Keck Cosmic Web Imager: a capable new integral field spectrograph for the W. M. Keck Observatory, Proc. SPIE 8446, 844613 (2012)
33. Murphy, M.T., Kacprzak, G.G., Savorgnan, G.A.D., Carswell, R.F.: The UVES Spectral Quasar Absorption Database (SQUAD) data release 1: the first 10 million seconds. MNRAS **482**, 3458–3479 (2019)
34. Nicastro, F., Confirming the Detection of two WHIM Systems along the Line of Sight to 1ES 1553+113, Proc. of the Vulcano Workshop 2018 - Frontier Objects in Astrophysics and Particle Physics, 20-26 May 2018, Frascati Physics Series, Vol. 66 (2018)
35. Nicastro, F., Kaastra, J., Krongold, Y., et al.: Observations of the missing baryons in the warm-hot intergalactic medium. Nature **558**, 406–409 (2018)
36. Nicastro, F., Krongold, Y., Mathur, S., Elvis, M.: A decade of warm hot intergalactic medium searches: Where do we stand and where do we go? AN **338**, 281–286 (2017)
37. O'Meara, J.M., Lehner, N., Howk, J.C., et al.: The First Data Release of the KODIAQ Survey. AJ **150**, 111 (2015)
38. Peeples, M. S., Corlies, L., Tumlinson, J., et al., Figuring Out Gas & Galaxies in Enzo (FOGGIE). I. Resolving Simulated Circumgalactic Absorption at $2 \leq z \leq 2.5$, ApJ, 873, 129 (2019)

39. Peeples, M.S., Werk, J.K., Tumlinson, J., et al.: A Budget and Accounting of Metals at z˜0: Results from the COS-Halos Survey. ApJ **786**, 54 (2014)
40. Persic, M., Salucci, P.: The baryon content of the universe. MNRAS **258**, 14P-18P (1992)
41. Planck Collaboration, Aghanim, N., Akrami, Y., Ashdown, et al., Planck 2018 results. VI. Cosmological parameters, A&A, 641, A6 (2020)
42. Prochaska, J.X., Burchett, J.N., Tripp, T.M., et al.: The COS Absorption Survey of Baryon Harbors: The Galaxy Database and Cross-correlation Analysis of O VI Systems. ApJS **243**, 24 (2019)
43. Prochaska, J.X., Zheng, Y.: Probing Galactic haloes with fast radio bursts. MNRAS **485**, 648–665 (2019)
44. Prochaska, J.X., Werk, J.K., Worseck, G., et al.: The COS-Halos Survey: Metallicities in the Low-redshift Circumgalactic Medium. ApJ **837**, 169 (2017)
45. Rauch, M.: The Lyman Alpha Forest in the Spectra of QSOs. ARA&A **36**, 267–316 (1998)
46. Richter, P., Fang, T., Bryan, G.L.: Simulations of thermally broadened H I Ly α absorption arising in the warm-hot intergalactic medium. A&A **451**, 767–776 (2006)
47. Richter, P., Savage, B.D., Sembach, K.R., Tripp, T.M.: Tracing baryons in the warm-hot intergalactic medium with broad Ly α absorption. A&A **445**, 827–842 (2006)
48. Sánchez-Janssen, R., Hammer, F., Morris, S., et al.: MOSAIC: the high multiplex and multi-IFU spectrograph for the ELT. Proc. SPIE **11447**, 1144725 (2020)
49. Shull, J. M., & Danforth, C. W., The Dispersion of Fast Radio Bursts from a Structured Intergalactic Medium at Redshifts z < 1.5, ApJL, 852, L11 (2018)
50. Shull, J.M., Smith, B.D., Danforth, C.W.: The Baryon Census in a Multiphase Intergalactic Medium: 30% of the Baryons May Still be Missing. ApJ **759**, 23 (2012)
51. Simcoe, R. A., Sargent, W. L. W., & Rauch, M., Characterizing the Warm-Hot Intergalactic Medium at High Redshift: A High-Resolution Survey for O VI at $z = 2.5$, ApJ, 578, 737-762 (2002)
52. Sutherland, R.S., Dopita, M.A.: Cooling Functions for Low-Density Astrophysical Plasmas. ApJS **88**, 253 (1993)
53. Tepper-García, T., Richter, P., Schaye, J., et al.: Absorption signatures of warm-hot gas at low redshift: broad H I Lyα absorbers. MNRAS **425**, 1640–1663 (2012)
54. Tilton, E.M., Danforth, C.W., Shull, J.M., Ross, T.L.: The Low-redshift Intergalactic Medium as Seen in Archival Legacy HST/STIS and FUSE Data. ApJ **759**, 112 (2012)
55. Tripp, T.M., Sembach, K.R., Bowen, D.V., et al.: A High-Resolution Survey of Low-Redshift QSO Absorption Lines: Statistics and Physical Conditions of O VI Absorbers. ApJS **177**, 39–102 (2008)
56. Tumlinson, J., Thom, C., Werk, J.K., et al.: The Large. Oxygen-Rich Halos of Star-Forming Galaxies Are a Major Reservoir of Galactic Metals, Sci **334**, 948 (2011)
57. Tuominen, T., Nevalainen, J., Tempel, E., et al.: An EAGLE view of the missing baryons. A&A **646**, A156 (2021)
58. Werk, J.K., Prochaska, J.X., Cantalupo, S., et al.: The COS-Halos Survey: Origins of the Highly Ionized Circumgalactic Medium of Star-Forming Galaxies. ApJ **833**, 54 (2016)
59. Werk, J.K., Prochaska, J.X., Tumlinson, J., et al.: The COS-Halos Survey: Physical Conditions and Baryonic Mass in the Low-redshift Circumgalactic Medium. ApJ **792**, 8 (2014)
60. Werk, J.K., Prochaska, J.X., Thom, C., et al.: The COS-Halos Survey: Keck LRIS and Magellan MagE Optical Spectroscopy. ApJS **198**, 3 (2012)
61. Zanutta, A., Atkinson, D., Baldini, V. et al. CUBES Phase-A design overview, ExA, in press as part of the CUBES Special Issue